

# Geophysical Research Letters<sup>®</sup>

## RESEARCH LETTER

10.1029/2022GL100100

### Key Points:

- Parsimonious and global models of daily transpiration in forests are identified from a pool of four models and 608 unique configurations
- Configurations based on simpler ET schemes (e.g., Priestley-Taylor) outperformed those based on more complex schemes (e.g., Penman-Monteith)
- Environmental constraints based on atmospheric moisture demand appear more effective than those based on soil moisture supply

### Supporting Information:

Supporting Information may be found in the online version of this article.

### Correspondence to:

R. M. Bright,  
[ryan.bright@nibio.no](mailto:ryan.bright@nibio.no)

### Citation:

Bright, R. M., Miralles, D. G., Poyatos, R., & Eisner, S. (2022). Simple models outperform more complex big-leaf models of daily transpiration in forested biomes. *Geophysical Research Letters*, 49, e2022GL100100. <https://doi.org/10.1029/2022GL100100>

Received 24 JUN 2022

Accepted 6 SEP 2022

### Author Contributions:

**Conceptualization:** Ryan M. Bright, Diego G. Miralles, Rafael Poyatos, Stephanie Eisner

**Data curation:** Rafael Poyatos

**Formal analysis:** Ryan M. Bright

**Funding acquisition:** Stephanie Eisner





**Investigation:** Ryan M. Bright, Diego G. Miralles, Rafael Poyatos, Stephanie Eisner

**Methodology:** Ryan M. Bright, Diego G. Miralles, Rafael Poyatos, Stephanie Eisner

© 2022. The Authors.

This is an open access article under the terms of the [Creative Commons Attribution-NonCommercial-NoDerivs License](https://creativecommons.org/licenses/by/4.0/), which permits use and distribution in any medium, provided the original work is properly cited, the use is non-commercial and no modifications or adaptations are made.

## Simple Models Outperform More Complex Big-Leaf Models of Daily Transpiration in Forested Biomes

Ryan M. Bright<sup>1</sup> , Diego G. Miralles<sup>2</sup> , Rafael Poyatos<sup>3,4</sup> , and Stephanie Eisner<sup>1</sup> 

<sup>1</sup>Department of Forests and Climate, Division of Forestry and Forest Resources, Norwegian Institute of Bioeconomy Research (NIBIO), Ås, Norway, <sup>2</sup>Hydro-Climate Extremes Lab (H-CEL), Department of the Environment, Ghent University, Ghent, Belgium, <sup>3</sup>CREAF, Cerdanyola del Vallès, Spain, <sup>4</sup>Universitat Autònoma de Barcelona, Cerdanyola del Vallès, Spain

**Abstract** Transpiration makes up the bulk of total evaporation in forested environments yet remains challenging to predict at landscape-to-global scales. We harnessed independent estimates of daily transpiration derived from co-located sap flow and eddy-covariance measurement systems and applied the triple collocation technique to evaluate predictions from big leaf models requiring no calibration. In total, four models in 608 unique configurations were evaluated at 21 forested sites spanning a wide diversity of biophysical attributes and environmental backgrounds. We found that simpler models that neither explicitly represented aerodynamic forcing nor canopy conductance achieved higher accuracy and signal-to-noise levels when optimally configured (rRMSE = 20%;  $R^2 = 0.89$ ). Irrespective of model type, optimal configurations were those making use of key plant functional type dependent parameters, daily LAI, and constraints based on atmospheric moisture demand over soil moisture supply. Our findings have implications for more informed water resource management based on hydrological modeling and remote sensing.

**Plain Language Summary** Forests comprise the largest share of Earth's vegetated surface area and play an integral role in its hydrological cycle. Forests transfer moisture from below the surface to the atmosphere via transpiration, affecting surface moisture budgets and weather patterns at local-to-regional scales. Our ability to accurately predict transpiration in forests is thus critical to reliable weather prediction and more informed water resource management. The most accurate predictions stem from process-oriented models with detailed representations of plant hydraulic architecture and leaf stomata regulation. These models, however, rely on inputs that are not widely available and thus are not well-suited for predictions across broader spatial scales. Here, we sought to identify models that could be readily applied using conventional input data streams to predict daily transpiration across a wide diversity of forested ecosystems and over large spatial scales. This was carried out by evaluating predictions emanating from four models of varying complexity against two independent estimates of daily transpiration. We found the most parsimonious models to be those requiring few meteorological variables and one forest structural variable as input, achieving an accuracy 33% higher and explaining 16% greater variance than the most complex models requiring additional meteorological and forest structural variables as input.

## 1. Introduction

Transpiration ( $T$ ) is the main component of terrestrial evaporation ( $E$ ) biologically controlled by plants and accounting for ~60% of  $E$  in global terrestrial ecosystems (Lian et al., 2018; Wei et al., 2017). Its quantification is important to study the effects of altered water supply or demand on terrestrial ecosystem functioning (Fisher et al., 2017), the relationship between terrestrial water and carbon cycling (Baldocchi, 1994; Ponton et al., 2006), the sensitivity of terrestrial ecosystems to climatic shifts (Good et al., 2017), and the role of terrestrial ecosystems in the global hydrological cycle (Schlesinger & Jasechko, 2014; van der Ent et al., 2010) and in the shaping of weather and climate (Miralles et al., 2014; Vergopolan & Fisher, 2016). Yet despite its relevance and scientific importance,  $T$  remains challenging to monitor and predict across large spatial scales, as evidenced by the large spread in  $T/E$  estimates emanating from climate models (25%–90%; Berg & Sheffield, 2019), hydrological models (31%–64%; Wei et al., 2017), and satellite-driven algorithms (24–76%; Miralles et al., 2016). Accurate and reliable predictions across large spatial scales are needed for more informed land use and water resource management (Fisher et al., 2017), yet often gains in accuracy occur at the expense of model parsimony and an increased dependence on input data that is difficult to acquire at these scales.

**Resources:** Rafael Poyatos  
**Supervision:** Diego G. Miralles  
**Visualization:** Ryan M. Bright  
**Writing – original draft:** Ryan M. Bright  
**Writing – review & editing:** Ryan M. Bright, Diego G. Miralles, Rafael Poyatos, Stephanie Eisner

Several approaches to model  $T$  exist. Many seek to constrain plant-atmosphere  $\text{CO}_2$  fluxes and water vapor exchange at the leaf level through the coupling of net  $\text{CO}_2$  assimilation rate and leaf stomatal conductance ( $g_s$ ), implying that  $T$  is tightly coupled with photosynthesis (Ball et al., 1987; Dickinson et al., 1998; Leuning, 1995). These carbon-coupled (CC) approaches vary widely in their sophistication and complexity, where the rate of photosynthesis can be based either on light use efficiency (Running et al., 2004) or biochemical models (Collatz et al., 1991; Farquhar et al., 1980), and where  $g_s$  and photosynthesis may either be based on empirical relationships or optimality theory where stomata act to maximize carbon gain while minimizing water loss (Cowan & Farquhar, 1977; G. Katul et al., 2010; Medlyn et al., 2011). Some CC approaches incorporate the physiology of plant hydraulic transport, with the most sophisticated approaches being those linking plant hydraulics to stomatal conductance with optimizations based on hydraulic risk (Y. Wang et al., 2020). CC approaches founded on principles of water-use efficiency, optimality theory, and hydraulic transport are, however, difficult to apply at large scale due to their reliance on several poorly known parameters or physical traits that vary substantially among different biomes and regions (Knauer et al., 2018; Mencuccini et al., 2019; Y. S. Lin et al., 2015). Further, optimality models including hydraulically enabled ones do not easily identify responses to vapor pressure and soil moisture deficits (Sabot et al., 2022).

These challenges motivate approaches to model  $T$  independently from photosynthesis (i.e., without carbon coupling) using information solely about the environmental state. These carbon-uncoupled (CU) approaches may be differentiated primarily by whether aerodynamic forcing and/or canopy conductance ( $G_c$ ) is explicitly represented (C. Lin et al., 2018). The modeling of  $G_c$  may in turn be differentiated by whether known physical phenomena are represented mechanistically (e.g. Launiainen et al., 2016; Leuning et al., 2008), or empirically (e.g. Jarvis et al., 1976). CU modeling approaches that neither explicitly consider aerodynamic forcing nor  $G_c$  embrace the concept that a defined transpiration rate under a given atmospheric demand and unlimited moisture supply or potential transpiration ( $T_p$ ) is reduced to  $T$  according to the state of the environment and the limits it imposes. Such limits are often manifested in these simpler CU models as multiplicative response functions to individual factors, assumed to be independent of each other. Although the number and type may vary, most embrace the concept of a soil moisture stress factor (Barton, 1979) or reduction function (Feddes & Raats, 2004) that quantifies the effect of soil water stress on plant water uptake (Miralles et al., 2011; Wu et al., 2021).

Carbon-uncoupled modeling approaches require many simplifications relative to those founded on principles of water-use efficiency, optimality theory, and hydraulic transport. While CU models are arguably more useful for large-scale application particularly those embracing the “big leaf” concept (Deardorff, 1978; K. Wang and Dickinson, 2012) there remains a large knowledge gap surrounding their optimal complexity; that is, the balance between gains in accuracy and large-scale applicability. CU models are often evaluated as a whole (Ershadi et al., 2014; McCabe et al., 2016; Miralles et al., 2016), with few efforts invested toward understanding the merits of the fundamental components underlying them. As one example, methods to apportion energy available ( $A$ ) for  $E$  into that driving  $T$  differ widely and may be based either on leaf area index (Launiainen et al., 2016; Leuning et al., 2008) or fractional vegetation coverage (Miralles et al., 2011; Mu et al., 2011) and further, may or may not consider whether any share of  $A$  is directed toward the evaporation of canopy intercepted moisture (Fisher et al., 2008; Mu et al., 2011). The impact of these methodological differences on predictive performance remains unclear. As another example, the value that various individual environmental constraints provide to a global model is also unclear. For instance, it has been posited that soil moisture (SM) supply may be less containing than atmospheric moisture demand in many biomes (Flo et al., 2021; Lu et al., 2022; Novick et al., 2016), suggesting that a constraint based on atmospheric demand (i.e., as vapor pressure deficit (VPD)) may be more effective than one based on SM for a model that is to be applied at the global scale. Complicating model evaluation further are the different ways of representing key behavior for the same individual stress (or constraint) functions, particularly for SM supply (Verhoef & Egea, 2014) and atmospheric moisture demand (C. Lin et al., 2018).

Here, our primary objective is to evaluate CU-based approaches for modeling  $T$  at the daily time step that are scalable globally using readily available input data sourced from satellite remote sensing, numerical weather forecasting, or climate model reanalysis streams and which do not require local calibration. We focus on forested ecosystems since these comprise the largest share of Earth's vegetated surface area (Potapov et al., 2022) and since climate warming-driven increases to atmospheric moisture demand will likely result in greater impacts on forests (Novick et al., 2016). Rather than evaluate specific off-the-shelf models as a whole, we embrace a modular approach that allows us to isolate some of their more distinguishing features and systematically evaluate their merits. This modular approach is particularly well-suited to evaluate the more empirically based CU modeling

approaches employing multiplicative factors since, by construct, these are meant to be independent of each other and, as such, should be evaluated on their skill to capture alone or in combination all the driving processes and constraints.

## 2. Methods and Data

### 2.1. Method Short Summary

We assess the predictive performance of 256 unique configurations of a model based on the Priestley and Taylor (1972) framework (henceforth PT), 256 unique configurations of a model based on the Milly and Dunne (2016) framework (henceforth MD), and 48 configurations each of two variants of the radiatively uncoupled Penman-Montieth framework (McColl, 2020; Monteith, 1965) in total 608 unique “big leaf” models of daily  $T$ , none of which are dependent on calibrated parameters. Our assessment relies on independent estimates of  $T$  obtained from collocated sap flow and eddy-covariance measurement systems, employed to estimate two model performance metrics based on the triple collocation (TC) technique (Gruber et al., 2016; McColl et al., 2014; Stoffelen, 1998) used in conjunction thereafter for model ranking. The advantage of TC is that it does not require a single reference data set to be considered as truth and thereby limits the effect of random and systematic errors of the two reference datasets (Gruber et al., 2020).

### 2.2. The Modular Approach

We configure model components or “modules” based on their intended purpose or functionality. For the PT and MD models, these modules include: (a) an empirical coefficient ( $\alpha$ ) either the ratio of potential to equilibrium evaporation (for PT) or the evaporative fraction (for MD); (b) transpiration apportioned  $A$  function(s); and (c) environmental stress/constraint function(s), where the latter includes an atmosphere moisture demand constraint ( $f_{VPD}$ ), a soil moisture supply constraint ( $f_{SM}$ ), a plant greenness constraint ( $f_G$ ), and a plant temperature constraint ( $f_T$ ). As for (a), adopted values are either the original universal values or the PFT-dependent values reported in Table 2 of Maes et al. (2019) ( $n = 2$  configurations). As for (b), the fraction of  $A$  apportioned to  $T$  or  $\lambda T_p/A$  is determined either as a function of canopy structure alone or both canopy structure and canopy dryness ( $n = 2$  configs.). As for (c), total environmental stress is determined as the product of either none or one of three  $f_{SM}$  functions, none or one of three  $f_{VPD}$  functions, none or one function for  $f_G$ , and none or one function for  $f_T$  ( $n = 64$  configs.).

For the two PM models, the modules include: (a) transpiration apportioned  $A$  function(s); (b) a  $G_c$  model; and (c) a soil moisture supply constraint. As for (a),  $\lambda T_p/A$  is determined either as a function of canopy structure or green canopy structure, or both (green) canopy structure and canopy dryness ( $n = 4$  configs.). As for (b), one of three carbon-uncoupled  $G_c$  models are applied. As for (c), either zero or one of three  $f_{SM}$  functions are applied ( $n = 4$  configs.).

Please refer to Sections S1 and S2 in Supporting Information S1 for full model details including details surrounding the  $G_c$  models,  $\lambda T_p/A$  functions, and all environmental stress/constraint functions. Key PFT-dependent parameters required as input to the constraint functions or  $G_c$  models (Table S2 in Supporting Information S1) are sourced from the comprehensive review by Hoshika et al. (2018).

### 2.3. Eddy-Covariance Data

We employ a LAI-based method to partition  $E$  into  $T$  given LAI's high power in explaining variation of  $T/E$  in time and space for a wide range of plant functional types and biomes (Burchard-Levine et al., 2021; Lian et al., 2018; L. Wang et al., 2014).

The empirical functions of Wei et al. (2017) are applied to obtain a second independent estimate of  $T$  or  $T_{EC}$  as:

$$T_{EC} = (\lambda E_{EC} a LAI_{EC}^b) CF^{-1} \quad (1)$$

where  $\lambda E_{EC}$  is the daily mean EC-derived ecosystem evaporation flux,  $CF$  is a factor ( $=28.4$ ) converting the daily latent heat flux (in  $W m^{-2}$ ) into a moisture flux (in  $mm d^{-1}$ ),  $LAI$  is a daily leaf area index, and  $a$  and  $b$  are PFT-dependent parameters. See Section S5 in Supporting Information S1 for data and method details surrounding the daily LAI input data set.

## 2.4. Sap Flow Data

Our third independent estimate of daily  $T$  is based on the upscaling of whole-tree sap flow in the SAPFLUXNET (SFN) database (Poyatos et al., 2021) to the stand level. First, sap flow from uncalibrated heat dissipation sensors is multiplied by 1.405 to account for known sap flow underestimation (Flo et al., 2019). Hourly whole-tree sap flow is first normalized per unit tree basal area, then averaged for each species at each site. Species-level sap flow per unit ground area is then estimated as the product of the species mean value of basal area-normalized sap flow and the total basal area occupied by that species in the stand. Then, species-level sap flow estimates are summed for all species, and the obtained value is rescaled to account for the basal area within the stand belonging to species whose sap flow was not measured. Finally, hourly stand-level sap flow is summed across all hours of the day to yield the daily sum, notated mathematically as:

$$T_{SF} \approx SF = \frac{BA}{\sum_{s=1}^{s=S} BA_s} \sum_{h=1}^{24} \sum_{s=1}^{s=S} BA_s \frac{1}{T} \sum_{t=1}^{t=T} \frac{SF_{h,s,t}}{BA_{s,t}} \quad (2)$$

where the transpiration flux ( $T_{SF}$ ) is approximated as a positive sap flow (SF), BA is the basal area of the stand ( $m^2$ ),  $BA_s$  is the basal area of species where sap flow is measured ( $m^2$ ),  $T$  is the total number of trees where sap flow is measured,  $S$  is the total number of species, and  $h$ ,  $s$ , and  $t$  are hour, species, and tree indices for measured trees, respectively.

## 2.5. Evaluation Sites

All sites in the SFN database where good spatial agreement exists between EC sites contained in the two syntheses datasets “FLUXNET15 version Feb. 2020” (Pastorello et al., 2020) and “ICOS Drought 18” (Drought 2018 Team and ICOS Ecosystem Thematic Centre, 2020) are selected for model evaluation. We limit the candidate EC sites only to those found in these two syntheses datasets since these data are well documented, have been processed using the same gap filling and energy balance correction methods, and have undergone numerous quality checks and vetting by the scientific community (Pastorello et al., 2020).

Only FLUXNET sites with tower locations <100 m away from sites in SFN are included in the analysis, resulting in 21 sites spanning five plant functional types, three biomes, nine climate zones, and an aridity index ( $P/E_p$ ) range of 0.63–1.8 (see Table S3 in Supporting Information S1). For sites that are found in both the FLUXNET15 and ICOS Drought 18 datasets, records are merged, and priority is given to the ICOS Drought 18 data for instances where overlap exists in the daily record between the two datasets. EC data falling outside the range defined by the temporal extent of the SFN record are discarded.

## 2.6. Model Evaluation via Triple Collocation

In total, 608 unique models are evaluated in the study, run (forced) with daily meteorological inputs sourced from the EC data set. For the latent heat flux ( $\lambda E_{EC}$ ) and for all requisite independent (model input) variables, days for which less than 80% of the sub-daily record are flagged as “measured” or “good quality gap-filled” are discarded. Given the diversity in model complexity and thus the span in the number of required model inputs additional filtering is carried out to ensure that model performance evaluation is not biased by discrepancies in the input record. In other words, for any given site, the non-discarded meteorological input record of the most complex model defines the daily record for which all models are subsequently applied. Model predictions yielding negative  $\lambda T$  values (owed to negative  $R_n - G$ ) are converted to zero. The resulting temporally synchronized and quality filtered EC-SFN record contains a total of 15,144 days.

We compute a TC-based root mean squared error (RMSE) and a squared correlation coefficient ( $\rho^2$ ) following the method of McColl et al. (2014), the latter of which informs about the correspondence between the model prediction and the two reference measurement system signals, and the degree to which they are in phase with each other. RMSE and  $\rho^2$  are computed for the full data set and six stratifications according to: (a) dryness based on a daily  $z_{api}$  threshold (see section S3 in Supporting Information S1; “Dry” = days with  $z_{api} < -0.5$ ; “Wet” = days with  $z_{api} \geq -0.5$ ); (b) phenology based on the leaf phenology of the dominant tree species at any given site (“EF” = evergreen forest; “DF” = deciduous forest); and (c) LAI based on the site maximum growing season LAI (i.e.,  $LAI_{max}$ ; “Low LAI” = all days for sites with  $LAI_{max} < 2.5 m^2 m^{-2}$ ; “High LAI” = all days for sites with  $LAI_{max} \geq 2.5 m^2 m^{-2}$ ).

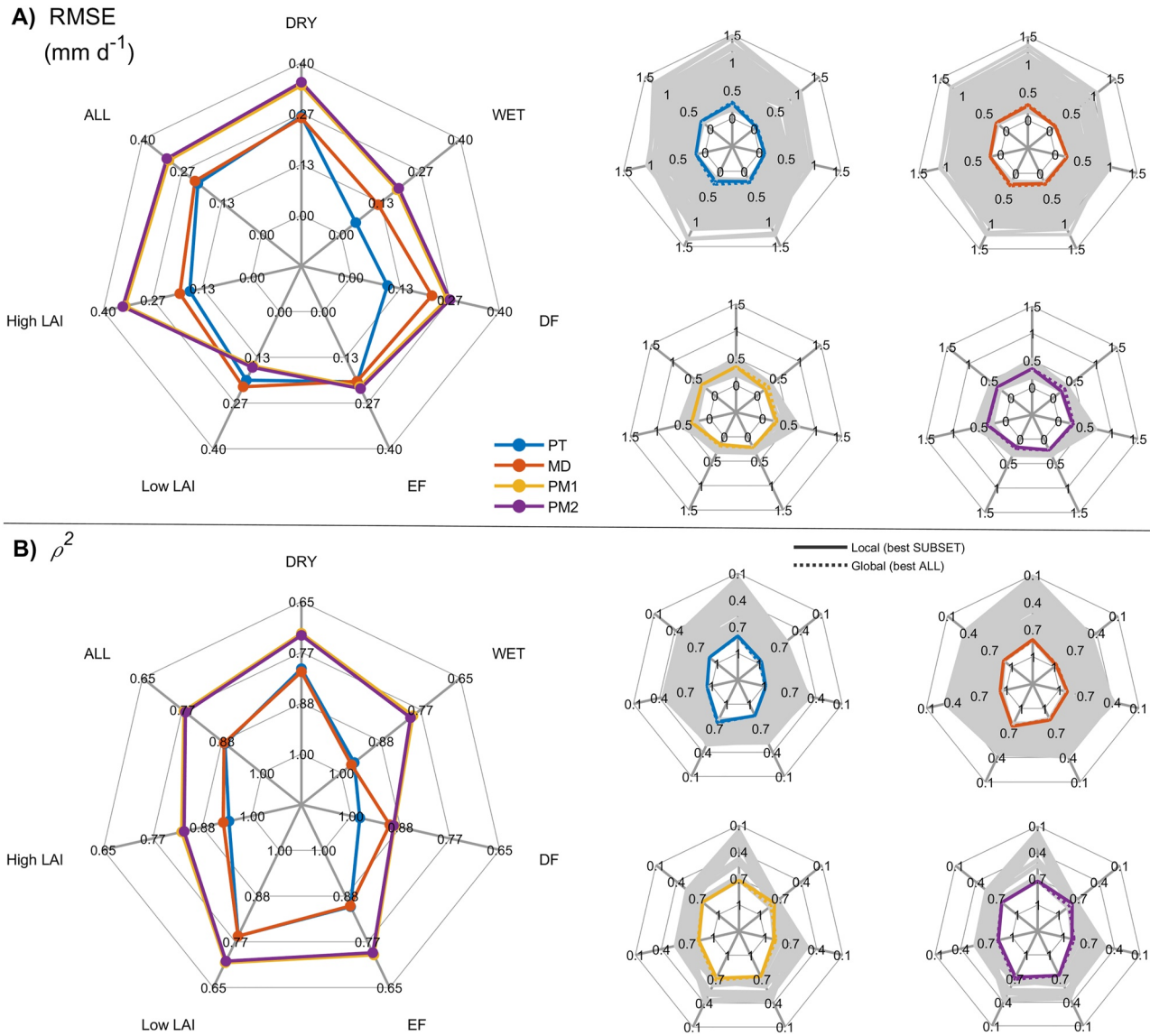


**Figure 1.** Performance metrics for the best model configuration by model type and data subset: (a) root mean squared error (RMSE); (b)  $\rho^2$ . Smaller subpanels at right show the best configurations (colored lines) in relation to all configurations (light gray lines).

A good model should have both high  $\rho^2$  and low RMSE. For each subset and for the full dataset, we identify the “best” model configuration for each model root scheme (i.e., PT, MD, PM1, and PM2) as that which yields the lowest sum of absolute differences between the minimum RMSE and maximum  $\rho^2$  realized after feature scaling (unity-based normalization).

### 3. Results

#### 3.1. Performance of Best Model Configurations

Figure 1 presents RMSE and  $\rho^2$  values for the best configuration of each model group for the six subsets and for the full data set, while Figure 2 provides the configuration details. In terms of RMSE (Figure 1a), the best MD and PT models notably outperformed the best PM models for the full data set and for the “Dry”, “Wet”, “DF”, and “High LAI” subsets, whereas for the “EF” subset RMSEs were similar across models. Only for the “Low LAI” subset did the two PM models outperform the MD and PT models. A deeper investigation into the latter revealed that the aerodynamic forcing during the shoulder seasons tended to increase in importance relative to the radiative

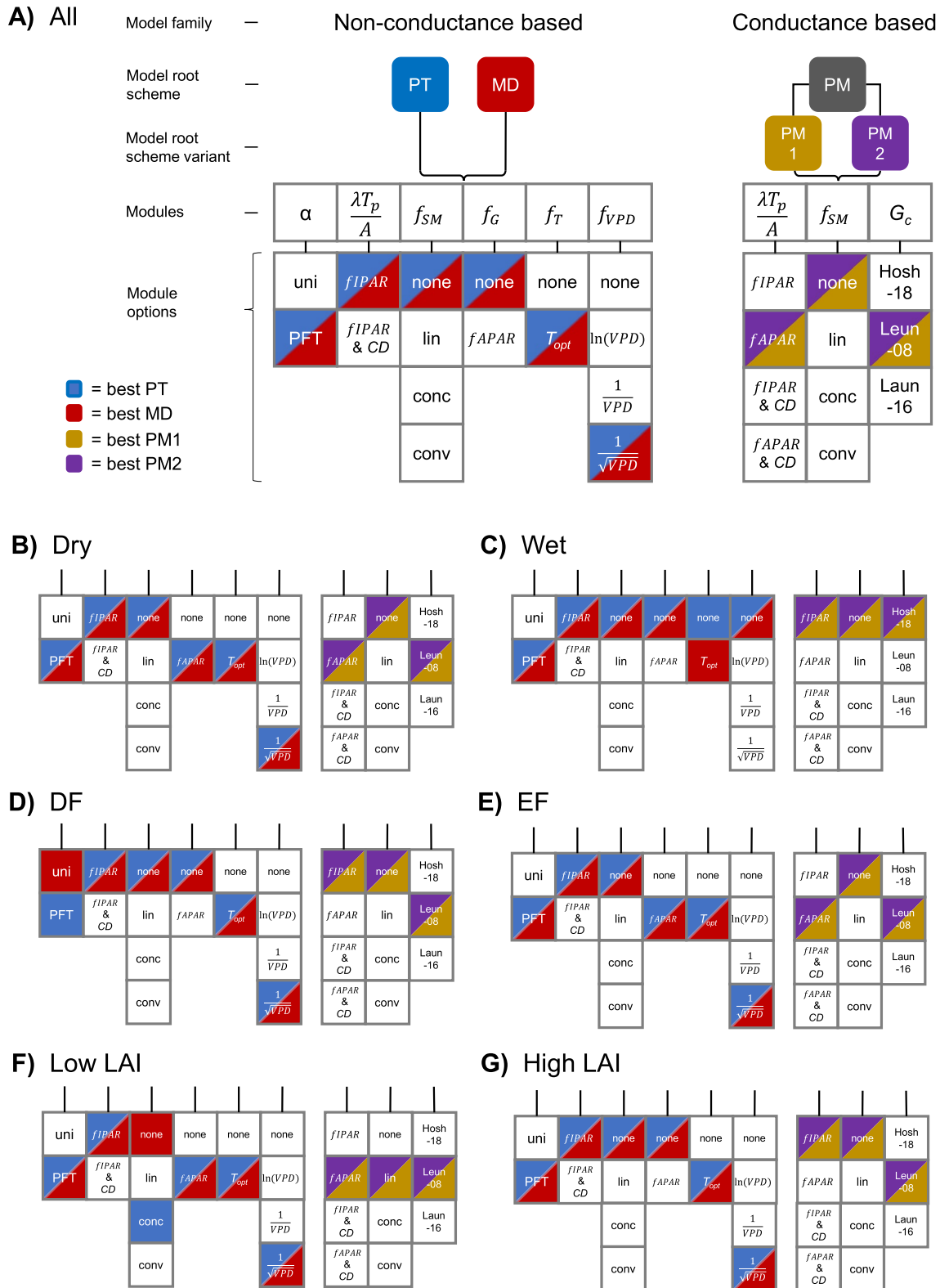


**Figure 2.** Best model configurations for the full data set (a) and for each subset (b–g).

forcing during peak growing season at the lower LAI sites, the former of which being better-captured by the PM models. Errors of the best MD and PT configurations were mostly similar across subsets with the exception of the “Wet”, “DF”, and “High LAI” subsets, where RMSEs of the best PT configurations were approximately 60%, 55%, and 14% lower than the best MD configurations, respectively (Figure 1a, blue vs. red). Over the full data set (Figure 1a, “All”) and considering a reference data set mean  $T$  of  $1.04 \text{ mm d}^{-1}$ , RMSEs for the best PT, MD, PM1, and PM2 configurations were 0.21 (20%), 0.22 (21%), 0.31 (30%), and 0.32 (31%)  $\text{mm d}^{-1}$ , respectively.

As for  $\rho^2$  (Figure 1b) or the signal-to-noise ratio (Gruber et al., 2020), the best PT and MD configurations yielded notably higher values than the best PM configurations across all subsets, with the exception of the “DF” subset where values for the two best PMs approximately equaled that of the best MD. Highest  $\rho^2$  values for all model groups were found at this subset, whereas the lowest values for all model groups were found at the “Low LAI” subset. Like RMSE, the best PT and MD configurations excelled at the “Wet” subset yielding  $\rho^2$  values as high as 0.96 and 0.97, respectively, though the highest  $\rho^2$  value seen of 0.98 emerged from the best PT configuration at the “DF” subset. Over the full dataset (Figure 1b, “All”), the best PT and MD configurations explained  $\sim 16\%$  greater variance than the best PM configurations.

### 3.2. Best Configuration Details

Figure 2 provides details about the configurations underlying the results presented in Section 3.1. The best configurations for both PM variants were found identical for the full data set and for each subset. The best MD and PT configurations were found identical to each other for the full data set (“All”) and for the “Dry”, “EF”, and “High LAI” subsets. For both the “Dry” (Figure 2b) and “EF” subsets (Figure 2e), the best MD and PT configurations made use of all environmental constraints apart from the soil moisture constraint ( $f_{SM}$ ), in addition to the PFT-dependent  $\alpha$  values and an available energy ( $A$ ) apportioning based on  $fIPAR$  alone. For these same two subsets, the soil moisture constraint was also absent from the best PM configurations employing the Leun-08  $G_c$  model, and  $A$  apportioning was based on  $fIPAR$  ( $=fIPAR \times f_G$ ) alone.

Contrary to the “Dry” subset, the environmental constraints were excluded from the best MD and PT configurations for the “Wet” subset, with the exception of the MD configuration which included the plant temperature constraint ( $f_T$ ; Figure 2c). Here, and only here the best PM configurations employed the Hosh-18  $G_c$  model, whereas for the rest of the subsets the Leun-08  $G_c$  model emerged in the best configurations of the two PM variants. For “Wet”, the best PM configurations also apportioned  $A$  based on  $fIPAR$  which is unsurprising given that  $f_G$  was not found to be useful here to the MD and PT models.

For the “DF” subset (Figure 2d), the best MD and PT configurations differed only by their  $\alpha$  values, where the best MD configuration employed the universal value of 0.8. This appeared to be the only subset in which the universal  $\alpha$  value was utilized in the best configuration of a non-conductance based model. The best MD and PT configurations also differed for the “Low LAI” subset (Figure 2f), where the best PT configuration made use of  $f_{SM}$  based on the concave stress model (Section S2, and Equation S15 in Supporting Information S1). The best PM configurations for “Low LAI” also made use of  $f_{SM}$  although here it was based on the linear stress model (Equation S14 in Supporting Information S1).

### 3.3. Local—Global Model Performance Trade-Offs

The configurations performing best over the full data set (“All”) emerged as best only for one or two subsets, suggesting that predictive performance under certain conditions (i.e., vegetation structure, phenology, aridity) is likely degraded when a global model is to be applied (Figure 2). To assess this performance degradation, we compared (Figure 1, sub-panels at right) performance measures for the best configurations for any given subset (henceforth referred to as “local”) against those of the model configuration performing best over the full data set (henceforth referred to as “global”).

In terms of RMSE (Figure 1a, right panels; Figure S8 in Supporting Information S1), trade-offs were generally largest for all models for the “Low LAI” subset, where the application of the best global configurations for PT, MD, PM1, and PM2 models led to RMSE increases of 0.06 (29%), 0.03 (13%), 0.03 (18%), and 0.03 (18%)  $\text{mm d}^{-1}$ , respectively, over the best local configurations. For both PMs, this increase could be attributed to the absence of the  $f_{SM}$  constraint, whereas for MD the increase could be attributed to the absence of the  $f_G$

constraint. For PT, the increase in RMSE could be attributed to the absence of both the  $f_G$  and  $f_{SM}$  constraints. Trade-offs in RMSE elsewhere for the PT and MD models were mostly negligible. For the PMs, however, we also detected non-negligible increases in RMSE for the “Wet” subset, where increases of 0.08 (41%) and 0.08 (39%)  $\text{mm d}^{-1}$  for the best global configurations of PM1 and PM2, respectively, could be attributed to use of the Leun-08  $G_c$  model over the Hosh-18  $G_c$  model, and use of  $f_{APAR}$  over  $f_{IPAR}$  as  $\lambda T_p/A$ .

In terms of  $\rho^2$  (Figure 1b, right panels), adverse non-negligible trade-offs (i.e.,  $\rho^2$  decreases) associated with deploying the best global over the best local configurations were mostly confined to the PM models for the “DF” and “Low LAI” subsets, where  $\rho^2$  decreases of  $-0.02$  ( $-3\%$ ) and  $-0.03$  ( $-3\%$ ) at “DF” and  $-0.03$  ( $-3\%$ ) and  $-0.03$  ( $-4\%$ ) at “Low LAI” were found for the PM1 and PM2 variants, respectively. Surprisingly, employing the best global over best local configurations of PM1 and PM2 for the “Wet” subset led to *increases* in  $\rho^2$  of 0.05 (6%) for both variants. This suggests that the best local PM configurations at “Wet” emerged as different to the best global configurations due to their greater gains in accuracy (reductions in RMSE) relative to reductions in  $\rho^2$ .

## 4. Discussion

### 4.1. Emergent Patterns

Clear patterns emerged surrounding the make-up of the best configurations (Figure 2). For the best non-conductance models, 13 of the 14 best configurations included the PFT-dependent  $\alpha$  values. While our study included some of the same EC sites ( $n = 9$ ) included in the source study (Maes et al., 2019), we do not believe this finding is undermined by this partial overlap as these sites only contributed to 21%, 35%, and 37% of the total number of days in the Maes et al. (2019) data subsets for ENF, DBF, and EBF forests, respectively (and 0% for both MF and SAV). An analysis of site-level results showed that many of our sites not included in the Maes et al. (2019) study benefitted from having PFT-dependent  $\alpha$  values. Another clear pattern emerging was that the  $f_{VPD}$  constraint appeared essential to the performance of these models, all of which were based on the  $VPD^{-0.5}$  model (Equation S13 in Supporting Information S1). Only for the “Wet” subset was the  $f_{VPD}$  constraint found absent in the best non-conductance model configurations. Further, the  $f_T$  constraint also emerged as vital to their performance, evidenced by their appearance in 13 of the 14 best configurations.

As for the conductance-based models, the Leun-08  $G_c$  model appeared in 12 of the 14 best configurations. This finding appears insensitive to the method applied to apportion  $A$  which varied across subsets.

Irrespective of model family, accounting for canopy dryness (CD) when apportioning  $A$  appeared unnecessary, even for the “Wet” subset. The same appeared to be true also for the  $f_{SM}$  constraint which was found beneficial to only 3 of the 28 total best model configurations.

### 4.2. Global Model Candidates

Across the full data set, the best PT and MD configurations yielded similar performance metrics that were far superior to the two best PM model configurations (Figure 1 “All”). Performance trade-offs between the best subset and “All” data set configurations for PT and MD were mostly negligible (Figure 1, right, “local” vs. “global”) which supports the use of the “All” configurations in global modeling contexts. Although their global configurations were identical, the structure of the  $E_p$  formulation underlying the best PT model was slightly more complex with its use of  $E_o$  fraction (i.e.,  $= \Delta/(\Delta + \gamma)$  in Equation S7 in Supporting Information S1) which depended on an additional meteorological input variable not required by the best MD configuration (i.e., air pressure in  $\gamma$ ). On the other hand, the best global configuration of the PT model gave notably better predictions in terms of both RMSE and  $\rho^2$  for three of six subsets, that is, under normal moisture conditions (“Wet”), in deciduous forests (“DF”), and in forests with high LAI (see Figure S8 in Supporting Information S1). Given this, it is hard to land on a single global model candidate among the two.

The best global PT and MD configurations yielded a daily RMSE of 0.21 and 0.22  $\text{mm d}^{-1}$ , respectively, which was roughly 20% and 21% of the combined mean daily  $T$  of the two reference datasets (i.e.,  $T_{SF}$  and  $T_{EC}$ ). Whether this is an acceptable error is challenging to discern given limited performance benchmarks for transpiration models reported in the literature which, arguably, is tied to the scarcity of transpiration observations. Indeed, this scarcity is a motivating factor behind the development of the SAPFLUXNET database (Poyatos et al., 2021) and hence its utilization in this study. While various models have been developed to



isolate  $T$  from EC-derived measurements of ecosystem  $E$  (Nelson et al., 2018; Perez-Priego et al., 2018; Zhou et al., 2016), use of such estimates in isolation as surrogate for a “true”  $T$  reference is fraught by the difficulties of dealing with both random and systematic errors (Eliasson et al., 2013; Gruber et al., 2020), to which the deployment of a second reference estimate and the triple collocation technique can serve to overcome (McColl et al., 2014; Miralles et al., 2010; Stoffelen, 1998). Nevertheless, for lack of other benchmarks and to provide additional perspective, a normalized RMSE of  $\sim 20\%$  across a diversity of forested sites ( $n = 21$ ) may be considered low when compared to those reported in Nelson et al. (2020) for individual sites based on comparison of  $T_{SF}$  and  $T$  derived from three different water flux partitioning methods (cf. Section 3.2 therein).

## 5. Conclusions

### 5.1. Summary of Key Findings

Our study revealed that simpler, non-conductance based models can perform remarkably well across a wide variety of forest types and conditions when adequately configured. The best MD and PT configurations greatly outperformed the best PM configurations in terms of both RMSE and  $\rho^2$  over the full data set and at most subsets (Figure 1), suggesting that  $T$  in global forests can be accurately modeled without explicit representations of canopy and aerodynamic conductances. Given the difficulties of obtaining reliable global-scale estimates of daily aerodynamic conductances, the noteworthiness of this finding can be appreciated.

A second notable finding is that the best model configurations tended to exclude a soil moisture stress constraint ( $f_{SM}$ ) in favor of a VPD constraint irrespective of the model family (Figure 2). We hypothesized that  $f_{SM}$  constraints were competing with VPD constraints, confirmed through additional examination of the relationship between  $f_{SM}$  and VPD constraints below the critical soil moisture stress threshold of  $-0.5 z_{API}$  (Section S8, Figures S6, and S7 in Supporting Information S1). The fact that VPD was sufficiently constraining supports findings reported elsewhere (Flo et al., 2021; Lu et al., 2022; Novick et al., 2016) about the relative importance of atmospheric moisture demand over soil moisture supply in constraining  $T$  in non-arid biomes.

A third was that there appeared to be little added benefit to the more complicated PM equation underlying PM2 relative to the standard formulation underlying PM1, at least when applied at the daily time step. The best PM1 and PM2 configurations were identical at each subset (Figure 2), and differences in performance measures between them were mostly negligible (Figures 1a and 1b). The purported strength of the modified PM equation of PM2 is that it does not break down in important limiting conditions (McColl, 2020), which may be more relevant at the sub-daily timescale.

### 5.2. Final Remarks

Over a wide range of forest ecosystems and environmental conditions, simple models of daily transpiration founded on a Milly & Dunne (2016) or Priestley & Taylor (1972) formulation of  $E_p$  yielded predictions that were  $\sim 33\%$  more accurate and explained  $\sim 16\%$  greater variance than more complex, physically based formulations based on the Penman-Monteith expression. These models required no calibration and relied solely on PFT-dependent parameters and widely available input variables, making them attractive candidates for global application. Indeed, a PT-based formulation has already been adopted by some satellite-based evapotranspiration algorithms (Fisher et al., 2008; Miralles et al., 2011). It is important to note that while PM performances might have been improved had we elected to re-calibrate key parameters of the  $G_c$  modules using data from our sites, such an exercise not only would have risked overfitting to a relatively sparse data set, but in doing so, could have compromised the integrity of the triple collocation analysis.

Findings reported here may be used to improve transpiration schemes employed in hydrological models and remote sensing algorithms, thus elevating the efficacy of water resource management measures that rely on predictions from such tools. The result that simple models are not only good but better at ecosystem scale makes hydrological assessments less data-intensive and thus more computationally efficient. Future efforts should be directed toward additional model vetting in forest ecosystems not well-covered by our data set, particularly those in arid regions as new observations based on sap flow or water flux partitioning approaches (Stoy et al., 2019) become available.

## Conflict of Interest

The authors declare no conflicts of interest relevant to this study.

## Data Availability Statement

The FLUXNET15 data set is available from: <https://fluxnet.org/data/fluxnet2015-dataset/>. The ICOS Drought 18 data set is available from: <https://www.icos-cp.eu/data-products>. The SAPFLUXNET data set is available from: <https://doi.org/10.5281/zenodo.3971689>. The LAI data set is available from: [https://daac.ornl.gov/cgi-bin/dsvviewer.pl?ds\\_id=1600](https://daac.ornl.gov/cgi-bin/dsvviewer.pl?ds_id=1600).

## Acknowledgments

R.M.B. and S.E. are supported by the Research Council of Norway, grant #295128. D.G.M. is supported by the European Research Council (ERC), grant #715254 (DRY-2-DRY). R.P. is supported by the Spanish State Research Agency (DATAFORUSE, RTI2018-095297-J-100) and the Alexander von Humboldt Foundation (Germany).

## References

- Baldocchi, D. (1994). A comparative study of mass and energy exchange rates over a closed C<sub>3</sub> (wheat) and an open C<sub>4</sub> (corn) crop: II. CO<sub>2</sub> exchange and water use efficiency. *Agricultural and Forest Meteorology*, 67(3), 291–321. [https://doi.org/10.1016/0168-1923\(94\)90008-6](https://doi.org/10.1016/0168-1923(94)90008-6)
- Ball, J. T., Woodrow, I. E., & Berry, J. A. (1987). A model predicting stomatal conductance and its contribution to the control of photosynthesis under different environmental conditions. In J. Biggins (Ed.), *Progress in photosynthesis Research: Volume 4 proceedings of the VIIIth international congress on photosynthesis providence, Rhode Island, USA* (pp. 221–224). Springer Netherlands.
- Barton, I. J. (1979). A parameterization of the evaporation from nonsaturated surfaces. *Journal of Applied Meteorology and Climatology*, 18(1), 43–47. [https://doi.org/10.1175/1520-0450\(1979\)018<0043:apotef>2.0.co;2](https://doi.org/10.1175/1520-0450(1979)018<0043:apotef>2.0.co;2)
- Berg, A., & Sheffield, J. (2019). Evapotranspiration partitioning in CMIP5 models: Uncertainties and future projections. *Journal of Climate*, 32(10), 2653–2671. <https://doi.org/10.1175/jcli-d-18-0583.1>
- Burchard-Levine, V., Nieto, H., Riaño, D., Kustas, W. P., Migliavacca, M., El-Madany, T. S., et al. (2021). A remote sensing-based three-source energy balance model to improve global estimations of evapotranspiration in semi-arid tree-grass ecosystems. *Global Change Biology*, 28(4), 1493–1515.
- Collatz, G. J., Ball, J. T., Grivet, C., & Berry, J. A. (1991). Physiological and environmental regulation of stomatal conductance, photosynthesis and transpiration: A model that includes a laminar boundary layer. *Agricultural and Forest Meteorology*, 54(2), 107–136. [https://doi.org/10.1016/0168-1923\(91\)90002-8](https://doi.org/10.1016/0168-1923(91)90002-8)
- Cowan, I. R., & Farquhar, G. D. (1977). Stomatal function in relation to leaf metabolism and environment. *Symposia of the Society for Experimental Biology*, 31, 471–505.
- Deardorff, J. W. (1978). Efficient prediction of ground surface temperature and moisture, with inclusion of a layer of vegetation. *Journal of Geophysical Research*, 83(C4), 1889–1903. <https://doi.org/10.1029/jc083ic04p01889>
- Dickinson, R. E., Shaikh, M., Bryant, R., & Graumlich, L. (1998). Interactive canopies for a climate model. *Journal of Climate*, 11(11), 2823–2836. [https://doi.org/10.1175/1520-0442\(1998\)011<2823:icfacm>2.0.co;2](https://doi.org/10.1175/1520-0442(1998)011<2823:icfacm>2.0.co;2)
- Drought 2018 Team and ICOS Ecosystem Thematic Centre. (2020). Drought-2018 ecosystem eddy covariance flux product for 52 stations in FLUXNET-Archive format. <https://doi.org/10.18160/YVR0-4898>
- Eliasson, S., Holl, G., Buehler, S. A., Kuhn, T., Stengel, M., Iturbide-Sanchez, F., & Johnston, M. (2013). Systematic and random errors between collocated satellite ice water path observations. *Journal of Geophysical Research: Atmospheres*, 118(6), 2629–2642. <https://doi.org/10.1029/2012jd018381>
- Ershadi, A., McCabe, M. F., Evans, J. P., Chaney, N. W., & Wood, E. F. (2014). Multi-site evaluation of terrestrial evaporation models using FLUXNET data. *Agricultural and Forest Meteorology*, 187, 46–61. <https://doi.org/10.1016/j.agrformet.2013.11.008>
- Farquhar, G. D., von Caemmerer, S., & Berry, J. A. (1980). A biochemical model of photosynthetic CO<sub>2</sub> assimilation in leaves of C<sub>3</sub> species. *Planta*, 149(1), 78–90. <https://doi.org/10.1007/bf00386231>
- Feddes, R. A., & Raats, P. A. C. (2004). Parameterizing the soil—Water—Plant root system. In R. A. Feddes, G. H. de Rooij, & J. C. van Dam (Eds.) *Unsaturated-zone modeling: Progress, challenges and applications* (pp. 95–141). Kluwer Academic Publishers.
- Fisher, J. B., Melton, F., Middleton, E., Hain, C., Anderson, M., Allen, R., et al. (2017). The future of evapotranspiration: Global requirements for ecosystem functioning, carbon and climate feedbacks, agricultural management, and water resources. *Water Resources Research*, 53(4), 2618–2626. <https://doi.org/10.1002/2016wr020175>
- Fisher, J. B., Tu, K. P., & Baldocchi, D. D. (2008). Global estimates of the land–atmosphere water flux based on monthly AVHRR and ISLSCP-II data, validated at 16 FLUXNET sites. *Remote Sensing of Environment*, 112(3), 901–919. <https://doi.org/10.1016/j.rse.2007.06.025>
- Flo, V., Martínez-Vilalta, J., Granda, V., Mencuccini, M., & Poyatos, R. (2021). Vapour pressure deficit is the main driver of tree canopy conductance across biomes. *Agricultural and Forest Meteorology*, 322, 109029. <https://doi.org/10.1016/j.agrformet.2022.109029>
- Flo, V., Martínez-Vilalta, J., Steppe, K., Schuldt, B., & Poyatos, R. (2019). A synthesis of bias and uncertainty in sap flow methods. *Agricultural and Forest Meteorology*, 271, 362–374. <https://doi.org/10.1016/j.agrformet.2019.03.012>
- Good, S. P., Moore, G. W., & Miralles, D. G. (2017). A mesic maximum in biological water use demarcates biome sensitivity to aridity shifts. *Nature Ecology & Evolution*, 1(12), 1883–1888. <https://doi.org/10.1038/s41559-017-0371-8>
- Gruber, A., De Lannoy, G., Albergel, C., Al-Yaari, A., Brocca, L., Calvet, J. C., et al. (2020). Validation practices for satellite soil moisture retrievals: What are the (the) errors? *Remote Sensing of Environment*, 244, 111806. <https://doi.org/10.1016/j.rse.2020.111806>
- Gruber, A., Su, C. H., Zwieback, S., Crow, W., Dorigo, W., & Wagner, W. (2016). Recent advances in (soil moisture) triple collocation analysis. *International Journal of Applied Earth Observation and Geoinformation*, 45, 200–211. <https://doi.org/10.1016/j.jag.2015.09.002>
- Hoshika, Y., Osada, Y., de Marco, A., Peñuelas, J., & Paoletti, E. (2018). Global diurnal and nocturnal parameters of stomatal conductance in woody plants and major crops. *Global Ecology and Biogeography*, 27(2), 257–275. <https://doi.org/10.1111/geb.12681>
- Katul, G., Manzoni, S., Palmroth, S., & Oren, R. (2010). A stomatal optimization theory to describe the effects of atmospheric CO<sub>2</sub> on leaf photosynthesis and transpiration. *Annals of Botany*, 105(3), 431–442. <https://doi.org/10.1093/aob/mcp292>
- Knauer, J., Zaehle, S., Medlyn, B. E., Reichstein, M., Williams, C. A., Migliavacca, M., et al. (2018). Towards physiologically meaningful water-use efficiency estimates from eddy covariance data. *Global Change Biology*, 24(2), 694–710. <https://doi.org/10.1111/geb.13893>
- Leuning, R. (1995). A critical appraisal of a combined stomatal-photosynthesis model for C<sub>3</sub> plants. *Plant, Cell and Environment*, 18(4), 339–355. <https://doi.org/10.1111/j.1365-3040.1995.tb00370.x>

- Lian, X., Piao, S., Huntingford, C., Li, Y., Zeng, Z., Wang, X., et al. (2018). Partitioning global land evapotranspiration using CMIP5 models constrained by observations. *Nature Climate Change*, 8(7), 640–646. <https://doi.org/10.1038/s41558-018-0207-9>
- Lin, Y.-S., Medlyn, B. E., Duursma, R. A., Prentice, I. C., Wang, H., Baig, S., et al. (2015). Optimal stomatal behaviour around the world. *Nature Climate Change*, 5(5), 459–464. <https://doi.org/10.1038/nclimate2550>
- Lu, H., Qin, Z., Lin, S., Chen, X., Chen, B., He, B., et al. (2022). Large influence of atmospheric vapor pressure deficit on ecosystem production efficiency. *Nature Communications*, 13(1), 1653. <https://doi.org/10.1038/s41467-022-29009-w>
- McCabe, M. F., Ershadi, A., Jimenez, C., Miralles, D. G., Michel, D., & Wood, E. F. (2016). The GEWEX LandFlux project: Evaluation of model evaporation using tower-based and globally gridded forcing data. *Geoscientific Model Development*, 9(1), 283–305. <https://doi.org/10.5194/gmd-9-283-2016>
- McCull, K. A., Vogelzang, J., Konings, A. G., Entekhabi, D., Piles, M., & Stoffelen, A. (2014). Extended triple collocation: Estimating errors and correlation coefficients with respect to an unknown target. *Geophysical Research Letters*, 41(17), 6229–6236. <https://doi.org/10.1002/2014gl061322>
- Mencuccini, M., Manzoni, S., & Christoffersen, B. (2019). Modelling water fluxes in plants: From tissues to biosphere. *New Phytologist*, 222(3), 1207–1222. <https://doi.org/10.1111/nph.15681>
- Miralles, D. G., Crow, W. T., & Cosh, M. H. (2010). Estimating spatial sampling errors in coarse-scale soil moisture estimates derived from point-scale observations. *Journal of Hydrometeorology*, 11(6), 1423–1429. <https://doi.org/10.1175/2010jhm1285.1>
- Miralles, D. G., Jimenez, C., Jung, M., Michel, D., Ershadi, A., McCabe, M. F., et al. (2016). The WACMOS-ET project—Part 2: Evaluation of global terrestrial evaporation data sets. *Hydrology and Earth System Sciences*, 20(2), 823–842. <https://doi.org/10.5194/hess-20-823-2016>
- Miralles, D. G., Teuling, A. J., van Heerwaarden, C. C., & Vilà-Guerau de Arellano, J. (2014). Mega-heatwave temperatures due to combined soil desiccation and atmospheric heat accumulation. *Nature Geoscience*, 7(5), 345–349. <https://doi.org/10.1038/ngeo2141>
- Nelson, J. A., Carvalhais, N., Cuntz, M., Delpierre, N., Knauer, J., Ogée, J., et al. (2018). Coupling water and carbon fluxes to constrain estimates of transpiration: The TEA algorithm. *Journal of Geophysical Research: Biogeosciences*, 123(12), 3617–3632. <https://doi.org/10.1029/2018jg004727>
- Nelson, J. A., Perez-Priego, O., Zhou, S., Poyatos, R., Zhang, Y., Blanken, P. D., et al. (2020). Ecosystem transpiration and evaporation: Insights from three water flux partitioning methods across FLUXNET sites. *Global Change Biology*, 26(12), 6916–6930. <https://doi.org/10.1111/gcb.15314>
- Novick, K. A., Ficklin, D. L., Stoy, P. C., Williams, C. A., Bohrer, G., & Oishi, A. C., (2016). The increasing importance of atmospheric demand for ecosystem water and carbon fluxes. *Nature Climate Change*, 6(11), 1023–1027.
- Pastorello, G., Trotta, C., Canfora, E., Chu, H., Christianson, D., Cheah, Y. W., et al. (2020). The FLUXNET2015 dataset and the ONEFlux processing pipeline for eddy covariance data. *Scientific Data*, 7(1), 225.
- Perez-Priego, O., Katul, G., Reichstein, M., El-Madany, T. S., Ahrens, B., Carrara, A., et al. (2018). Partitioning eddy covariance water flux components using physiological and micrometeorological approaches. *Journal of Geophysical Research: Biogeosciences*, 123(10), 3353–3370. <https://doi.org/10.1029/2018jg004637>
- Ponton, S., Flanagan, L. B., Alstad, K. P., Johnson, B. G., Morgenstern, K., Kljun, N., et al. (2006). Comparison of ecosystem water-use efficiency among Douglas-fir forest, aspen forest and grassland using eddy covariance and carbon isotope techniques. *Global Change Biology*, 12(2), 294–310. <https://doi.org/10.1111/j.1365-2486.2005.01103.x>
- Potapov, P., Hansen, M. C., Pickens, A., Hernandez-Serna, A., Tyukavina, A., Turubanova, S., et al. (2022). The global 2000–2020 land cover and land use change dataset derived from the landsat archive: First results. *Frontiers in Remote Sensing*, 3, 856903. <https://doi.org/10.3389/frsen.2022.856903>
- Running, S. W., Nemani, R. R., Heinsch, F. A., Zhao, M., Reeves, M., & Hashimoto, H. (2004). A continuous satellite-derived measure of global terrestrial primary production. *BioScience*, 54(6), 547–560. [https://doi.org/10.1641/0006-3568\(2004\)054\[0547:acsmog\]2.0.co;2](https://doi.org/10.1641/0006-3568(2004)054[0547:acsmog]2.0.co;2)
- Sabot, M. E. B., De Kauwe, M. G., Pitman, A. J., Medlyn, B. E., Ellsworth, D. S., Martin-StPaul, N. K., et al. (2022). One stomatal model to rule them all? Toward improved representation of carbon and water exchange in global models. *Journal of Advances in Modeling Earth Systems*, 14(4), e2021MS002761. <https://doi.org/10.1029/2021ms002761>
- Schlesinger, W. H., & Jasechko, S. (2014). Transpiration in the global water cycle. *Agricultural and Forest Meteorology*, 189–190, 115–117. <https://doi.org/10.1016/j.agrformet.2014.01.011>
- Stoffelen, A. (1998). Toward the true near-surface wind speed: Error modeling and calibration using triple collocation. *Journal of Geophysical Research*, 103(C4), 7755–7766. <https://doi.org/10.1029/97jc03180>
- Stoy, P. C., El-Madany, T. S., Fisher, J. B., Gentine, P., Gerken, T., Good, S. P., et al. (2019). Reviews and syntheses: Turning the challenges of partitioning ecosystem evaporation and transpiration into opportunities. *Biogeosciences*, 16(19), 3747–3775. <https://doi.org/10.5194/bg-16-3747-2019>
- van der Ent, R. J., Savenije, H. H. G., Schaeffli, B., & Steele-Dunne, S. C. (2010). Origin and fate of atmospheric moisture over continents. *Water Resources Research*, 46(9). <https://doi.org/10.1029/2010wr009127>
- Vergopolan, N., & Fisher, J. B. (2016). The impact of deforestation on the hydrological cycle in Amazonia as observed from remote sensing. *International Journal of Remote Sensing*, 37(22), 5412–5430. <https://doi.org/10.1080/01431161.2016.1232874>
- Verhoef, A., & Egea, G. (2014). Modeling plant transpiration under limited soil water: Comparison of different plant and soil hydraulic parameterizations and preliminary implications for their use in land surface models. *Agricultural and Forest Meteorology*, 191, 22–32. <https://doi.org/10.1016/j.agrformet.2014.02.009>
- Wang, K., & Dickinson, R. E. (2012). A review of global terrestrial evapotranspiration: Observation, modeling, climatology, and climatic variability. *Review of Geophysics*, 50(2), RG2005. <https://doi.org/10.1029/2011rg000373>
- Wang, L., Good, S. P., & Caylor, K. K. (2014). Global synthesis of vegetation control on evapotranspiration partitioning. *Geophysical Research Letters*, 41(19), 6753–6757. <https://doi.org/10.1002/2014gl061439>
- Wang, Y., Sperry, J. S., Anderegg, W. R. L., Venturas, M. D., & Trugman, A. T. (2020). A theoretical and empirical assessment of stomatal optimization modeling. *New Phytologist*, 227(2), 311–325. <https://doi.org/10.1111/nph.16572>
- Wu, X., Shi, J., Zuo, Q., Zhang, M., Xue, X., Wang, L., et al. (2021). Parameterization of the water stress reduction function based on soil–plant water relations. *Irrigation Science*, 39(1), 101–122. <https://doi.org/10.1007/s00271-020-00689-w>
- Zhang, Y., Chiew Francis, H. S., Peña-Arancibia, J., Sun, F., Li, H., & Leuning, R. (2017). Global variation of transpiration and soil evaporation and the role of their major climate drivers. *Journal of Geophysical Research: Atmospheres*, 122(13), 6868–6881. <https://doi.org/10.1002/2017jd027025>
- Zhou, S., Yu, B., Zhang, Y., Huang, Y., & Wang, G. (2016). Partitioning evapotranspiration based on the concept of underlying water use efficiency. *Water Resources Research*, 52(2), 1160–1175. <https://doi.org/10.1002/2015wr017766>

## References From the Supporting Information

- Ali, S., Ghosh, N. C., & Singh, R. (2010). Rainfall–runoff simulation using a normalized antecedent precipitation index. *Hydrological Sciences Journal*, 55(2), 266–274. <https://doi.org/10.1080/02626660903546175>
- Caird, M. A., Richards, J. H., & Donovan, L. A. (2007). Nighttime stomatal conductance and transpiration in C<sub>3</sub> and C<sub>4</sub> plants. *Plant Physiology*, 143(1), 4–10. <https://doi.org/10.1104/pp.106.092940>
- Carrão, H., Russo, S., Sepulcre-Canto, G., & Barbosa, P. (2016). An empirical standardized soil moisture index for agricultural drought assessment from remotely sensed data. *International Journal of Applied Earth Observation and Geoinformation*, 48, 74–84. <https://doi.org/10.1016/j.jag.2015.06.011>
- Daley, M. J., & Phillips, N. G. (2006). Interspecific variation in nighttime transpiration and stomatal conductance in a mixed New England deciduous forest. *Tree Physiology*, 26(4), 411–419. <https://doi.org/10.1093/treephys/26.4.411>
- Damour, G., Simonneau, T., Cochard, H., & Urban, L. (2010). An overview of models of stomatal conductance at the leaf level. *Plant, Cell and Environment*, 33(9), 1419–1438. <https://doi.org/10.1111/j.1365-3040.2010.02181.x>
- Dawson, T. E., Burgess, S. S. O., Tu, K. P., Oliveira, R. S., Santiago, L. S., Fisher, J. B., et al. (2007). Nighttime transpiration in woody plants from contrasting ecosystems. *Tree Physiology*, 27(4), 561–575. <https://doi.org/10.1093/treephys/27.4.561>
- Friedl, M. A., McIver, D., Hodges, J., Zhang, X., Muchoney, D., Strahler, A., et al. (2002). Global land cover mapping from MODIS: Algorithms and early results. *Remote Sensing of Environment*, 83(1–2), 287–302. [https://doi.org/10.1016/S0034-4257\(02\)00078-0](https://doi.org/10.1016/S0034-4257(02)00078-0)
- Grossiord, C., Buckley, T. N., Cernusak, L. A., Novick, K. A., Poulter, B., Siegwolf, R. T. W., et al. (2020). Plant responses to rising vapor pressure deficit. *New Phytologist*, 226(6), 1550–1566. <https://doi.org/10.1111/nph.16485>
- Jarvis, P. G., Monteith, J. L., & Weatherley, P. E. (1976). The interpretation of the variations in leaf water potential and stomatal conductance found in canopies in the field. *Philosophical Transactions of the Royal Society of London B Biological Sciences*, 273(927), 593–610.
- June, T. J. R. E., & Farquhar, G. D. (2004). A simple new equation for the reversible temperature dependence of photosynthetic electron transport: A study on soybean leaf. *Functional Plant Biology*, 31(3), 275–283. <https://doi.org/10.1071/fp03250>
- Katul, G. G., Palmroth, S., & Oren, R. (2009). Leaf stomatal responses to vapour pressure deficit under current and CO<sub>2</sub>-enriched atmosphere explained by the economics of gas exchange. *Plant, Cell and Environment*, 32(8), 968–979. <https://doi.org/10.1111/j.1365-3040.2009.01977.x>
- Kelliher, F. M., Leuning, R., Raupach, M. R., & Schulze, E. D. (1995). Maximum conductances for evaporation from global vegetation types. *Agricultural and Forest Meteorology*, 73(1–2), 1–16. [https://doi.org/10.1016/0168-1923\(94\)02178-m](https://doi.org/10.1016/0168-1923(94)02178-m)
- Kohler, M. A., & Linsley, R. K. (1951). *Predicting the runoff from storm rainfall* Rep. US Department of Commerce, Weather Bureau. 30.
- Krueger, E. S., Ochsner, T. E., & Qiring, S. M. (2019). Development and evaluation of soil moisture-based indices for agricultural drought monitoring. *Agronomy Journal*, 111(3), 1392–1406. <https://doi.org/10.2134/ajonj2018.09.0558>
- Launiainen, S., Katul Gabriel, G., Kolari, P., Lindroth, A., Lohila, A., Aurela, M., et al. (2016). Do the energy fluxes and surface conductance of boreal coniferous forests in Europe scale with leaf area? *Global Change Biology*, 22(12), 4096–4113. <https://doi.org/10.1111/gcb.13497>
- Leeper, R. D., Petersen, B., Palecki, M. A., & Diamond, H. (2021). Exploring the use of standardized soil moisture as a drought indicator. *Journal of Applied Meteorology and Climatology*, 60(8), 1021–1033. <https://doi.org/10.1175/jamc-d-20-0275.1>
- Leuning, R., Zhang, Y. Q., Rajaud, A., Cleugh, H. A., & Tu, K. (2008). A simple surface conductance model to estimate regional evaporation using MODIS leaf area index and the Penman-Monteith equation. *Water Resources Research*, 44(10). <https://doi.org/10.1029/2007wr006562>
- Li, X., Wei, Y., & Li, F. (2021). Optimality of antecedent precipitation index and its application. *Journal of Hydrology*, 595, 126027. <https://doi.org/10.1016/j.jhydrol.2021.126027>
- Lin, C., Gentine, P., Huang, Y., Guan, K., Kimm, H., & Zhou, S. (2018). Diel ecosystem conductance response to vapor pressure deficit is suboptimal and independent of soil moisture. *Agricultural and Forest Meteorology*, 250–251, 24–34. <https://doi.org/10.1016/j.agrformet.2017.12.078>
- Lohammar, T., Larsson, S., Linder, S., & Falk, S. O. (1980). FAST: Simulation models of gaseous exchange in Scots pine. *Ecological Bulletins*, 505–523.
- Maes, W. H., Gentine, P., Verhoest, N. E. C., & Miralles, D. G. (2019). Potential evaporation at eddy-covariance sites across the globe. *Hydrology and Earth System Sciences*, 23(2), 925–948. <https://doi.org/10.5194/hess-23-925-2019>
- Maruyama, A., & Kuwagata, T. (2008). Diurnal and seasonal variation in bulk stomatal conductance of the rice canopy and its dependence on developmental stage. *Agricultural and Forest Meteorology*, 148(6), 1161–1173. <https://doi.org/10.1016/j.agrformet.2008.03.001>
- McColl, K. A. (2020). Practical and theoretical benefits of an alternative to the Penman-Monteith evapotranspiration equation. *Water Resources Research*, 56(6), e2020WR027106. <https://doi.org/10.1029/2020wr027106>
- Medlyn, B. E., Duursma, R. A., Eamus, D., Ellsworth, D. S., Prentice, I. C., Barton, C. V. M., et al. (2011). Reconciling the optimal and empirical approaches to modelling stomatal conductance. *Global Change Biology*, 17(6), 2134–2144. <https://doi.org/10.1111/j.1365-2486.2010.02375.x>
- Michel, D., Jimenez, C., Miralles, D. G., Jung, M., Hirschi, M., Ershadi, A., et al. (2016). The WACMOS-ET project—Part 1: Tower-scale evaluation of four remote-sensing-based evapotranspiration algorithms. *Hydrology and Earth System Sciences*, 20(2), 803–822. <https://doi.org/10.5194/hess-20-803-2016>
- Milly, P. C. D., & Dunne, K. A. (2016). Potential evapotranspiration and continental drying. *Nature Climate Change*, 6(10), 946–949. <https://doi.org/10.1038/nclimate3046>
- Miralles, D. G., Holmes, T. R. H., De Jeu, R. A. M., Gash, J. H., Meesters, A. G. C. A., & Dolman, A. J. (2011). Global land-surface evaporation estimated from satellite-based observations. *Hydrology and Earth System Sciences*, 15(2), 453–469. <https://doi.org/10.5194/hess-15-453-2011>
- Monsi, M., & Saeki, T. (2005). On the factor light in plant communities and its importance for Matter production. *Annals of Botany*, 95(3), 549–567. <https://doi.org/10.1093/aob/mci052>
- Monteith, J. L. (1965). Evaporation and environment. *Symposia of the Society for Experimental Biology*, 19, 205–224.
- Mu, Q., Zhao, M., & Running, S. W. (2011). Improvements to a MODIS global terrestrial evapotranspiration algorithm. *Remote Sensing of Environment*, 115(8), 1781–1800. <https://doi.org/10.1016/j.rse.2011.02.019>
- Myneni, B. R., Knyazikhin, Y., & Park, T. (2015). MCD15A2HMODIS/Terra+AquaLeafAreaIndex/FPAR8-dayL4Global500mSINgridV006. <https://doi.org/10.5067/MODIS/MCD15A2H.006>
- Oren, R., Sperry, J. S., Katul, G. G., Pataki, D. E., Ewers, B. E., Phillips, N., & Schäfer, K. V. R. (1999). Survey and synthesis of intra- and interspecific variation in stomatal sensitivity to vapour pressure deficit. *Plant, Cell and Environment*, 22(12), 1515–1526. <https://doi.org/10.1046/j.1365-3040.1999.00513.x>
- ORNL DAAC. (2018). *MODIS and VIIRS land product subsets RESTful web service*. ORNL DAAC. <https://doi.org/10.3334/ORNLDAAC/1600>
- Peel, M. C., Finlayson, B. L., & McMahon, T. A. (2007). Updated world map of the Köppen-Geiger climate classification. *Hydrology and Earth System Sciences*, 11(5), 1633–1644. <https://doi.org/10.5194/hess-11-1633-2007>
- Pellarin, T., Louvet, S., Gruhier, C., Quantin, G., & Legout, C. (2013). A simple and effective method for correcting soil moisture and precipitation estimates using AMSR-E measurements. *Remote Sensing of Environment*, 136, 28–36. <https://doi.org/10.1016/j.rse.2013.04.011>

- Pellarin, T., Tran, T., Cohard, J. M., Galle, S., Laurent, J. P., de Rosnay, P., & Viscel, T. (2009). Soil moisture mapping over West Africa with a 30 min temporal resolution using AMSR-E observations and a satellite-based rainfall product. *Hydrology and Earth System Sciences*, 13(10), 1887–1896. <https://doi.org/10.5194/hess-13-1887-2009>
- Poyatos, R., Granda, V., Flo, V., Adams, M. A., Adorján, B., Aguadé, D., et al. (2021). Global transpiration data from sap flow measurements: The SAPFLUXNET database. *Earth System Science Data*, 13(6), 2607–2649.
- Priestley, C. H. B., & Taylor, R. J. (1972). On the assessment of surface heat flux and evaporation using large-scale parameters. *Monthly Weather Review*, 100(2), 81–92. [https://doi.org/10.1175/1520-0493\(1972\)100<0081:otaosh>2.3.co;2](https://doi.org/10.1175/1520-0493(1972)100<0081:otaosh>2.3.co;2)
- Ramsauer, T., Weiß, T., Löw, A., & Marzahn, P. (2021). RADOLAN\_API: An hourly soil moisture data set based on weather radar, soil properties and reanalysis temperature data. *Remote Sensing*, 13(9), 1712. <https://doi.org/10.3390/rs13091712>
- Reis, M. G. D., & Ribeiro, A. (2020). Conversion factors and general equations applied in agricultural and forest meteorology.
- Resco de Dios, V., Chowdhury, F. I., Granda, E., Yao, Y., & Tissue, D. T. (2019). Assessing the potential functions of nocturnal stomatal conductance in C<sub>3</sub> and C<sub>4</sub> plants. *New Phytologist*, 223(4), 1696–1706. <https://doi.org/10.1111/nph.15881>
- Schoener, G., & Stone, M. C. (2020). Monitoring soil moisture at the catchment scale—A novel approach combining antecedent precipitation index and radar-derived rainfall data. *Journal of Hydrology*, 589, 125155. <https://doi.org/10.1016/j.jhydrol.2020.125155>
- Sharpe, P. J. H. (1973). Adaxial and abaxial stomatal resistance of cotton in the Field. *Agronomy Journal*, 65(4), 570–574. <https://doi.org/10.2134/agronj1973.00021962006500040014x>
- Vallis, G. K., Parker, D. J., & Tobias, S. M. (2019). A simple system for moist convection: The rainy–Bénard model. *Journal of Fluid Mechanics*, 862, 162–199. <https://doi.org/10.1017/jfm.2018.954>
- Veberič, D. (2012). Lambert W function for applications in physics. *Computer Physics Communications*, 183(12), 2622–2628. <https://doi.org/10.1016/j.cpc.2012.07.008>
- Wei, Z., Yoshimura, K., Wang, L., Miralles, D. G., Jasechko, S., & Lee, X. (2017). Revisiting the contribution of transpiration to global terrestrial evapotranspiration. *Geophysical Research Letters*, 44(6), 2792–2801. <https://doi.org/10.1002/2016gl072235>
- Went, F. W. (1953). The effect of temperature on plant growth. *Annual Review of Plant Physiology*, 4(1), 347–362. <https://doi.org/10.1146/annurev.pp.04.060153.002023>
- Willmott, C. J., & Matsuura, K. (2001). Terrestrial air temperature and precipitation: Monthly and annual time series (1950–1999). Retrieved from [http://climate.geog.udel.edu/~climate/html\\_pages/README\\_ghcn\\_ts2.html](http://climate.geog.udel.edu/~climate/html_pages/README_ghcn_ts2.html)
- Xu, M., Hu, J., Zhang, T., Wang, H., Zhu, X., Wang, J., et al. (2021). Specific responses of canopy conductance to environmental factors in a coniferous plantation in subtropical China. *Ecological Indicators*, 131, 108168. <https://doi.org/10.1016/j.ecolind.2021.108168>
- Yu, K., Goldsmith, G. R., Wang, Y., & Anderegg, W. R. L. (2019). Phylogenetic and biogeographic controls of plant nighttime stomatal conductance. *New Phytologist*, 222(4), 1778–1788. <https://doi.org/10.1111/nph.15755>
- Zeppel, M. J. B., Lewis, J. D., Phillips, N. G., & Tissue, D. T. (2014). Consequences of nocturnal water loss: A synthesis of regulating factors and implications for capacitance, embolism and use in models. *Tree Physiology*, 34(10), 1047–1055. <https://doi.org/10.1093/treephys/tpu089>
- Zeri, M., Williams, K., Cunha, A. P. M. A., Cunha-Zeri, G., Vianna, M. S., Blyth, E. M., et al. (2021). Importance of including soil moisture in drought monitoring over the Brazilian semiarid region: An evaluation using the JULES model, in situ observations, and remote sensing. *Climate Resilience and Sustainability*. <https://doi.org/10.1002/cli2.7>
- Zhang, L., Hu, Z., Fan, J., Zhou, D., & Tang, F. (2014). A meta-analysis of the canopy light extinction coefficient in terrestrial ecosystems. *Frontiers of Earth Science*, 8(4), 599–609. <https://doi.org/10.1007/s11707-014-0446-7>
- Zhang, Y., Leuning, R., Hutley Lindsay, B., Beringer, J., McHugh, I., & Walker Jeffrey, P. (2010). Using long-term water balances to parameterize surface conductances and calculate evaporation at 0.05° spatial resolution. *Water Resources Research*, 46(5). <https://doi.org/10.1029/2009wr008716>
- Zhang, Y., Pena-Arancibia, J. L., McVicar, T. R., Chiew, F. H. S., Vaze, J., Liu, C., et al. (2016). Multi-decadal trends in global terrestrial evapotranspiration and its components. *Scientific Reports*, 6(1), 19124. <https://doi.org/10.1038/srep19124>